Electronic Supplementary Material (ESI) for ChemComm.

Supplementary Information

MoS_2/graphene cathodes for reversibly storing Mg^{2+} and Mg^{2+}/Li^+ in rechargeable magnesium-anode batteries

Cheng-Jui Hsu,[a,b] Chih-Yu Chou,[b] Cheng-Hsien Yang,[a] Tai-Chou Lee,[b]

Jeng-Kuei Chang*,[a,b,c]

[a] Institute of Materials Science and Engineering, National Central University, Taiwan

[b] Department of Chemical and Materials Engineering, National Central University, Taiwan

[c] Department of Mechanical Engineering, National Central University, Taiwan

Experimental details

MoS_2 powder (99%) was purchased from Alfa Aesar and used as received. The carbon nanotubes (CNTs) (Nanostructured & Amorphous Materials; 99%) had outer and inner diameters of approximately 30 and 10 nm, respectively, and a length of 5–15 μm. Graphene nanosheets (GNSs) were prepared using a modified Staudenmaier method. Natural graphite powder (Alfa Aesar; particle size: ~70 μm; purity: 99.999%) was chemically oxidized to form graphite oxide (GO) at room temperature. The graphite (5 g) was continuously stirred in a mixed solution of sulfuric acid (100 mL), nitric acid (50 mL), and potassium chlorate (50 g) for ~100 h. The resulting GO was rinsed with a 5 wt.% HCl aqueous solution and then repeatedly washed with deionized water until the pH of the filtrate became neutral. The product was dried in air and pulverized. Finally, the GO was exfoliated by rapid heating (~30 °C/min) to 1100 °C under an inert Ar atmosphere. After thermal reduction (held at 1100 °C for 30 min), GNSs were obtained.

A ball-milling machine (SPEX 8000D) was used to mix MoS_2 with CNTs and GNSs (10 wt.%); the ball-to-powder weight ratio was 7:3. All the materials were weighed and handled in a N_2-filled glove box. After being sealed under the inert atmosphere, the ball-milling vessel was transferred to the milling machine. The milling time was 30 min.

The microstructures of the samples were examined using scanning electron microscopy (SEM; FEI Inspect F50) and transmission electron microscopy (TEM; JEOL 2100). X-ray photoelectron spectroscopy (XPS; VG Sigma Probe) and energy-dispersive X-ray spectroscopy (EDS; Bruker XFlash) were employed to study the chemical composition. X-ray diffraction (XRD; Bruker D2 Phaser, with a Cu target)

was used to analyze the material crystallinity.

To prepare an electrode, a slurry, comprising 70 wt.% active material, 20 wt.% carbon black, and 10 wt.% poly(vinylidene fluoride) in *N*-methyl-2-pyrrolidone solution, was pasted onto Ni foil and vacuum-dried at 80 °C for 8 h. This electrode was then punched to match the required dimension (i.e., 1.3 cm in diameter) of a CR2032 coin cell. Mg foil and a glassy fiber membrane were used as the counter electrode and the separator, respectively. All-phenyl-complex (APC) electrolytes, containing 0.4 M phenylmagnesium chloride (PhMgCl), 0.2 M aluminum chloride ($AlCl_3$), and anhydrous tetrahydrofuran (THF) solvent, with various LiCl concentrations were used. Assembly of the coin cell was performed in an argon-filled glove box (Innovation Technology Co.), where both the moisture content and oxygen content were maintained at below 0.1 ppm. Cyclic voltammetry (CV) measurements were performed using a Biologic VSP-300 potentiostat in the range of 0.1–1.8 V. The charge–discharge performance (in terms of capacity, high-rate capability, and cyclic stability) of the cells was evaluated at 25 °C with an Arbin BT-2043 battery tester.

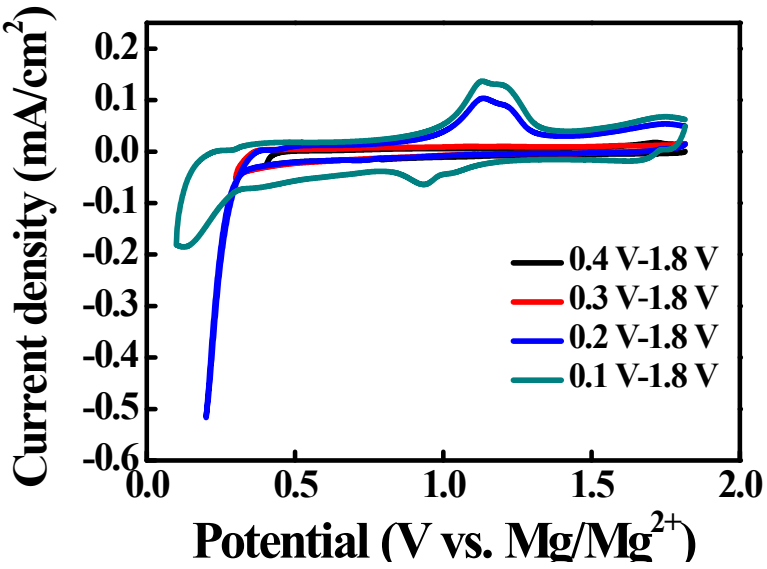

Figure S1. CV curves of MoS_2 electrode recorded in Li^+-containing APC electrolyte. Potential was scanned from 1.8 V to various lower limits with sweep rate of 0.1 mV/s. Results indicate that 2H-MoS_2 (before phase transformation at ~0.2 V) was inactive in this electrolyte.

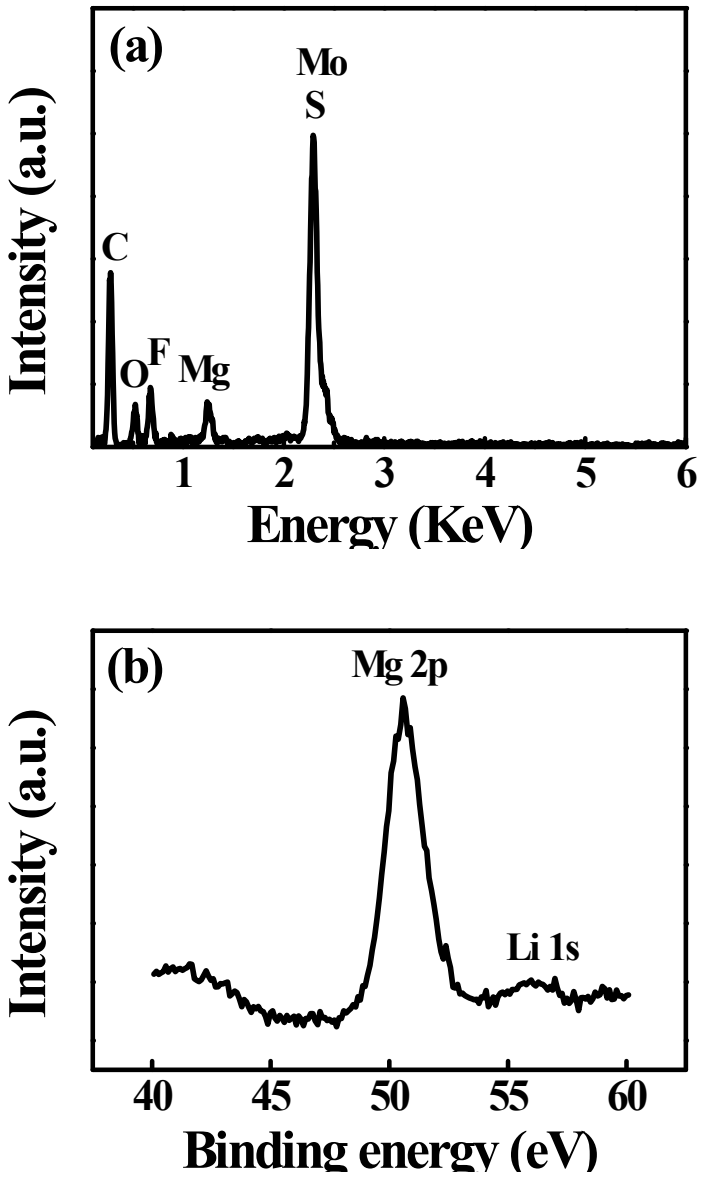

Figure S2. (a) EDS and (b) XPS analyses of MoS_2 electrode after being discharged to 0.1 V.

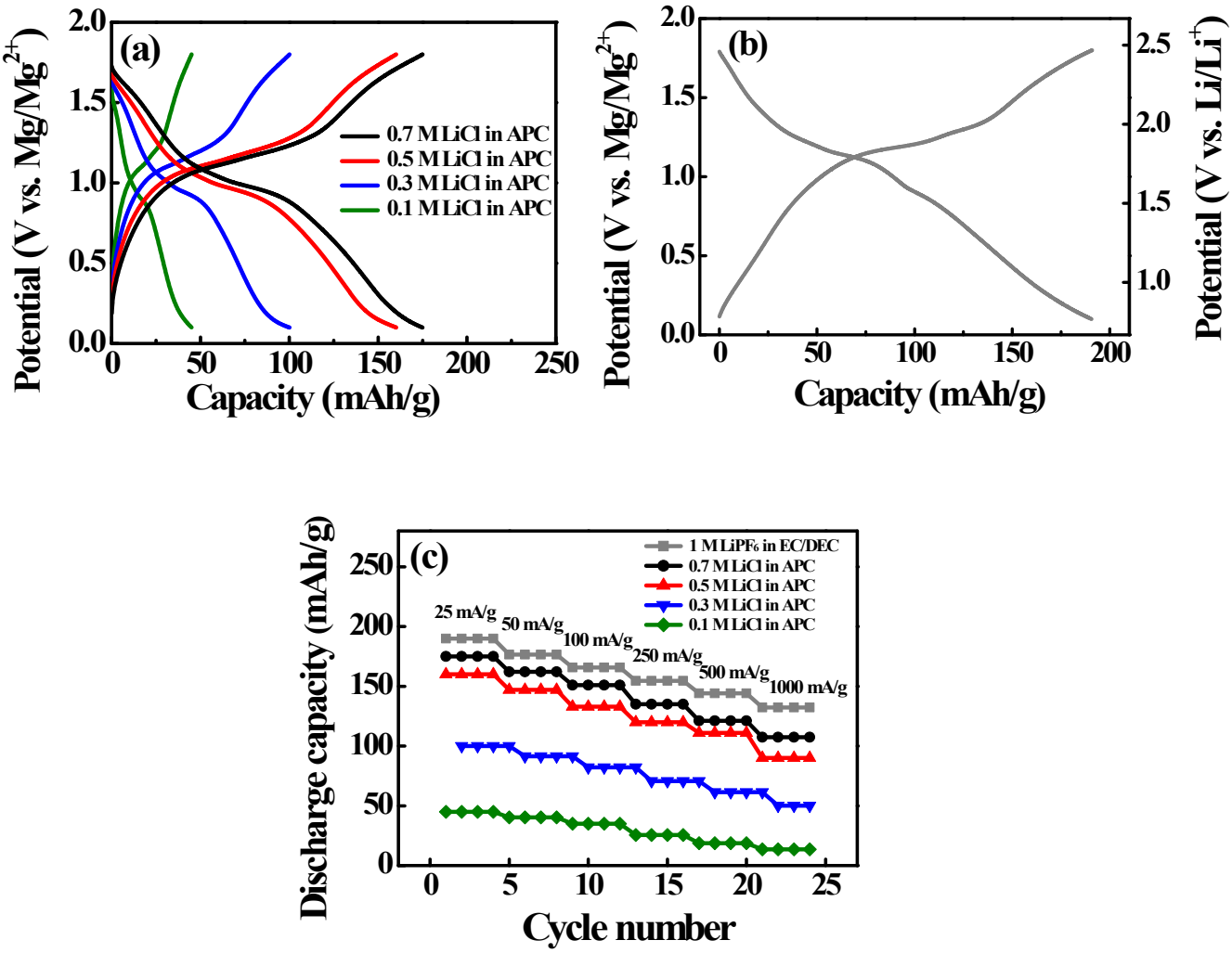

Figure S3. (a) Charge–discharge curves of MoS_2 electrode recorded in APC electrolytes with various LiCl concentrations. (b) Charge–discharge curves of MoS_2 electrode recorded in 1 M $LiPF_6$/ethylene carbonate–diethyl carbonate electrolyte (with a Li counter). (c) Rate capability of MoS_2 electrode in various electrolytes.

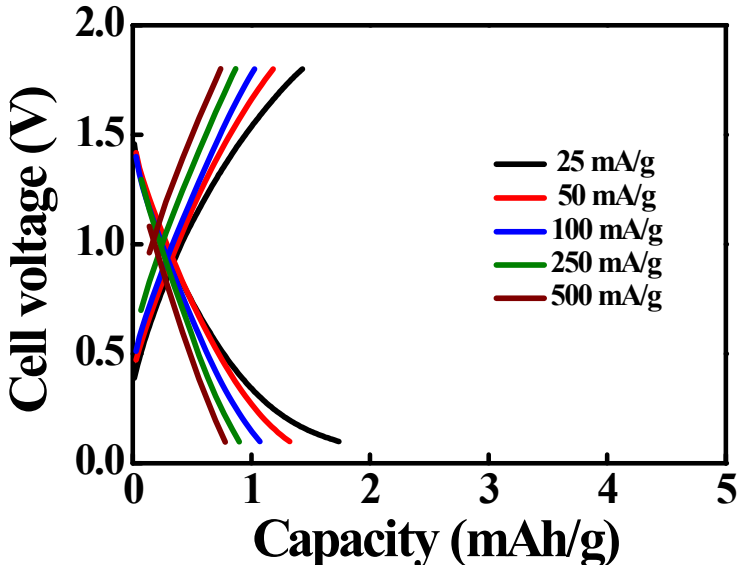

Figure S4. Charge–discharge curves of fresh MoS_2 electrode recorded in plain APC electrolyte (without Li^+).

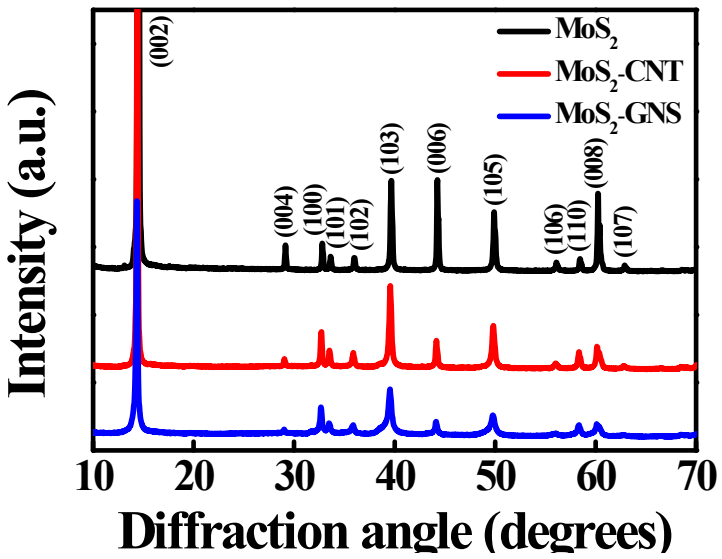

Figure S5. XRD patterns of as-received MoS_2, MoS_2-CNT, and MoS_2-GNS samples.

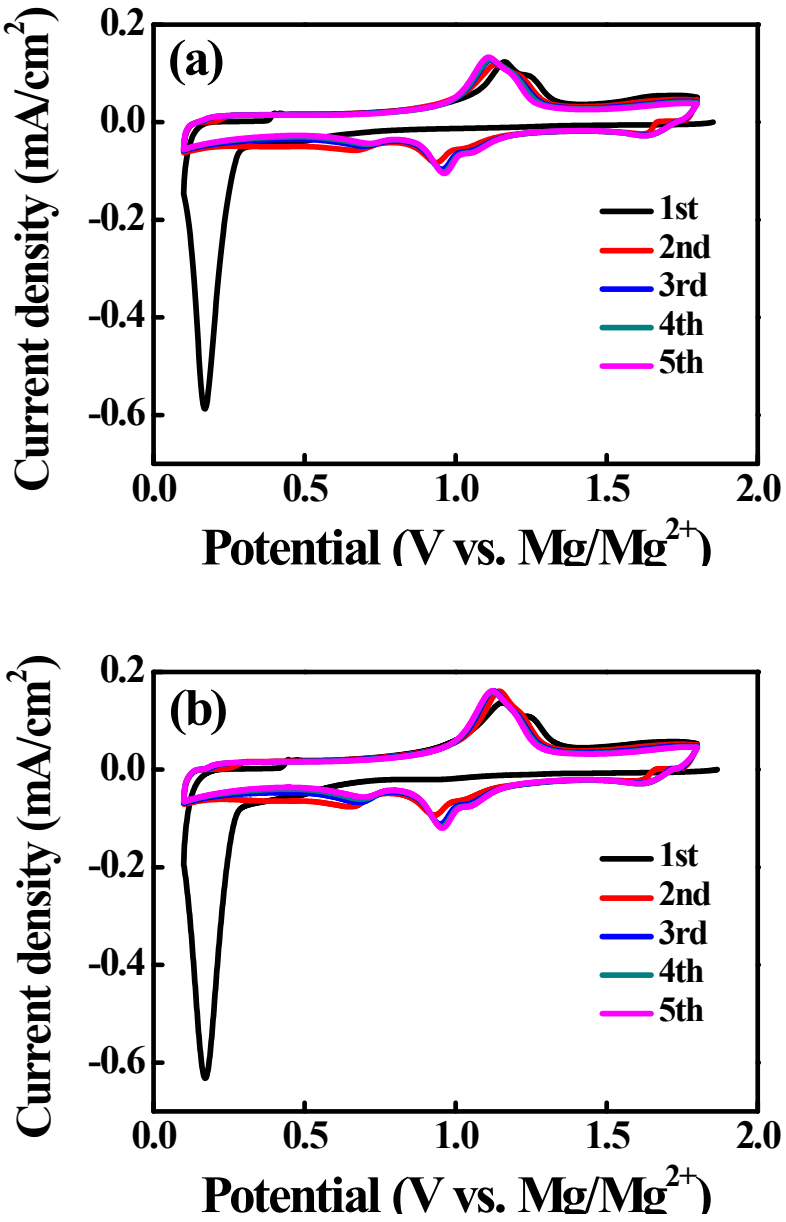

Figure S6. CV curves of (a) MoS_2-CNT and (b) MoS_2-GNS electrodes recorded in Li^+-containing APC electrolyte with potential sweep rate of 0.1 mV/s.

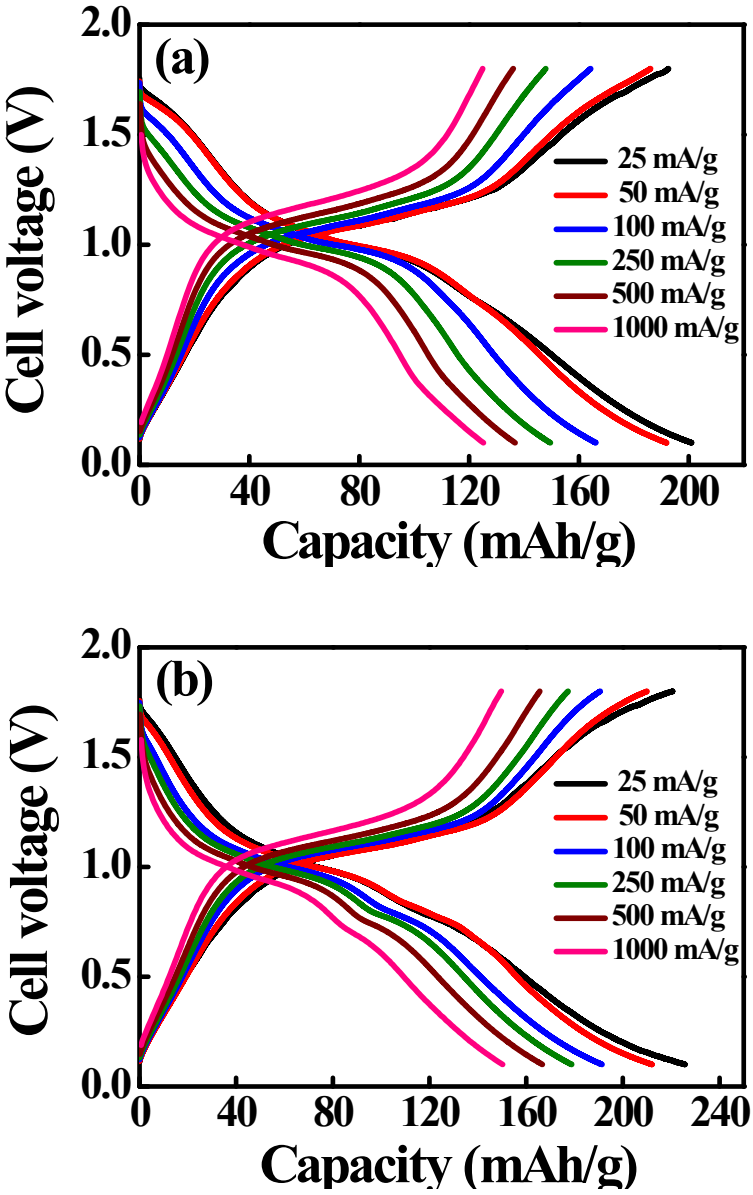

Figure S7. Charge–discharge curves of (a) MoS_2-CNT and (b) MoS_2-GNS electrodes recorded in Li^+-containing APC electrolyte with various current densities.

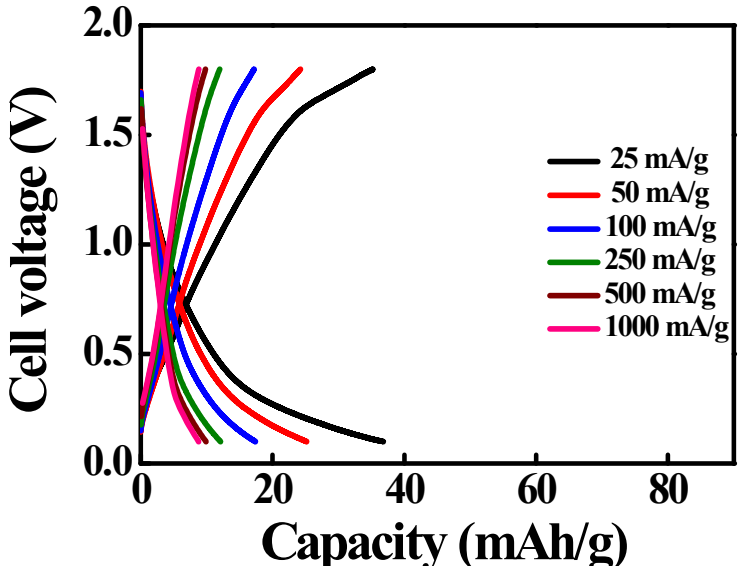

Figure S8. Charge–discharge curves of plain GNS electrode recorded in Li^+-containing APC electrolyte with various current densities.

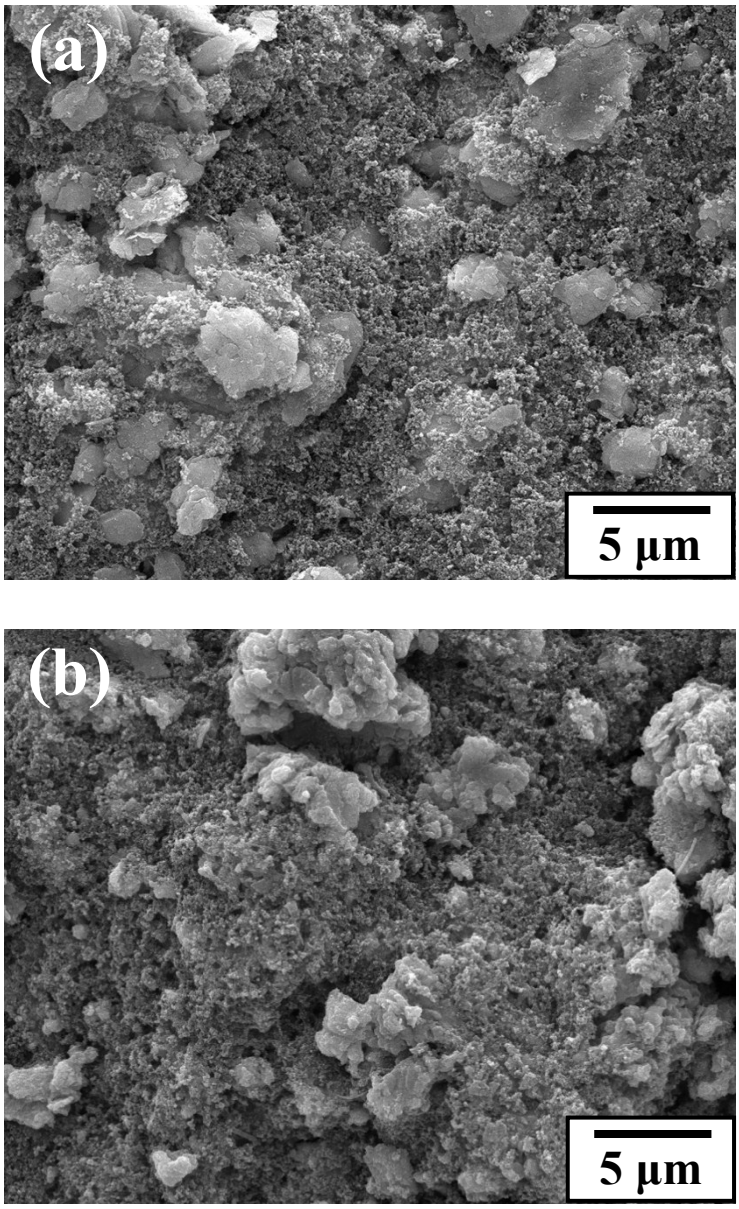

Figure S9. SEM micrographs of MoS_2-GNS electrode before and after being tested in Li^+-containing APC electrolyte for 200 charge–discharge cycles.